Journal of Photochemistry and Photobiology A: Chemistry 260 (2013) 9–13

Contents lists available at SciVerse ScienceDirect

Journal of Photochemistry and Photobiology A: Chemistry

journal homepage: www.elsevier.com/locate/jphotochem

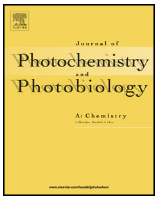

A porphyrin molecule that generates, traps, stores, and releases singlet oxygen

Chuchawin Changtong[a], Daniel W. Carney[a], Lan Luo[a], Christopher A. Zoto[a], John L. Lombardi[b], Robert E. Connors[a,*]

[a] *Department of Chemistry and Biochemistry, Worcester Polytechnic Institute, Worcester, MA 01609, USA*
[b] *Ventana Research Corporation, Tucson, AZ 85713, USA*

ARTICLE INFO

Article history:
Received 1 February 2013
Received in revised form 7 March 2013
Accepted 10 March 2013
Available online 21 March 2013

Keywords:
Singlet oxygen
Photosensitizer
Porphyrin

ABSTRACT

Tetraphenylporphyrin (H2TPP), covalently linked to four 2-pyridone moieties was synthesized (**II**) and studied. This composite molecule, in combination with light and ground state oxygen, has the ability to generate, trap, store, and release singlet oxygen. The process can be operated reversibly without detectable decomposition or side reactions using light with wavelength greater than 500 nm. Oxidation of the target molecule, 2-chloroethyl ethyl sulfide (CEES), by singlet oxygen released from the endoperoxide of the porphyrin-2-pyridone molecule (**I**) is demonstrated. Spectroscopic and kinetic data do not reveal evidence of perturbation between the porphyrin and pyridone ring systems of **II**. The decomposition kinetics for the endoperoxide adduct **I** are first order with activation parameters $\Delta H\ddagger = 26.7$ (kcal/mol) and $\Delta G\ddagger = 24.0$ (kcal/mol). Experimental and computational studies of unattached N-benzyl-2-pyridone peroxide are reported and compared to the experimental data for **I**.

1. Introduction

It is well known that the $^1\Delta_g$ excited state of oxygen, referred to as singlet oxygen, shows chemical reactivity that differs significantly from that of ground state $^3\Sigma^-{}_g$ molecular oxygen. This has led to a range of applications for singlet oxygen that include photodynamic therapy (PDT), water purification, novel chemical synthesis, and chemical/biological decontamination [1,2]. Singlet oxygen is commonly generated by the transfer of energy from a photosensitizer dye to a $^3\Sigma^-{}_g$ oxygen molecule. The process is initiated when light promotes the sensitizer to its first excited singlet state which then undergoes intersystem crossing to populate the lowest triplet state. Singlet oxygen is produced when the triplet state of the sensitizer transfers energy to ground state oxygen. Depending upon the solvent, singlet oxygen decays back to the ground state with a half-life ($\tau_{1/2}$) in the range of 10^{-6}–10^{-2} s. [3]. Other molecules (M) in solution may be oxidized if they react with singlet oxygen before it deactivates to $^3\Sigma^-{}_g$. These processes are summarized below.

$$\text{Sens} + h\nu \rightarrow {}^1\text{Sens} \rightarrow {}^3\text{Sens}$$

$$^3\text{Sens} + O_2(^3\Sigma^-{}_g) \rightarrow \text{Sens} + O_2(^1\Delta_g)$$

$$O_2(^1\Delta_g) \rightarrow O_2(^3\Sigma^-{}_g)$$

$$M + O_2(^1\Delta_g) \rightarrow \text{Oxidized products}$$

Previous work has established that a number of organic ring compounds are capable of reversibly trapping and storing singlet oxygen with high efficiency by forming endoperoxides as oxidation products [4]. These storage endoperoxides decompose to the original molecule by releasing oxygen in the excited $^1\Delta_g$ state which, as noted, has stronger oxidizing properties than O_2 in its triplet ground state [1]. Matsumoto et al. [5] has shown that a series of N-substituted 2-pyridones form endoperoxides that yield singlet oxygen in high yield upon thermal decomposition. The first-order thermolysis reactions have $\tau_{1/2} = 2$–6 h at 40 °C for the 2-pyridones studied [5]. The work presented here describes the preparation and several physical and chemical properties of a composite molecule that has four 2-pyridone moieties that store singlet oxygen bonded directly to a porphyrin photosensitizer dye. These materials, under the action of light and oxygen, have the capacity to generate, trap, store, and release singlet oxygen (Fig. 1). ^{1}H NMR reveals that this cycle can be repeated a number of times without detectable degradation or formation of side products. Unlike conventional photosensitization methods to produce singlet oxygen, the reversible storage capacity of these materials ensures that singlet oxygen will continue to be generated for hours after the excitation light source has been removed. Spectroscopic and kinetic properties have been measured and theoretically modeled for this novel compound. In addition, oxidation of the mustard gas

---

* Corresponding author. Tel.: +1 508 831 5394.
E-mail address: rconnors@wpi.edu (R.E. Connors).

1010-6030/$ – see front matter © 2013 Elsevier B.V. All rights reserved.
http://dx.doi.org/10.1016/j.jphotochem.2013.03.003

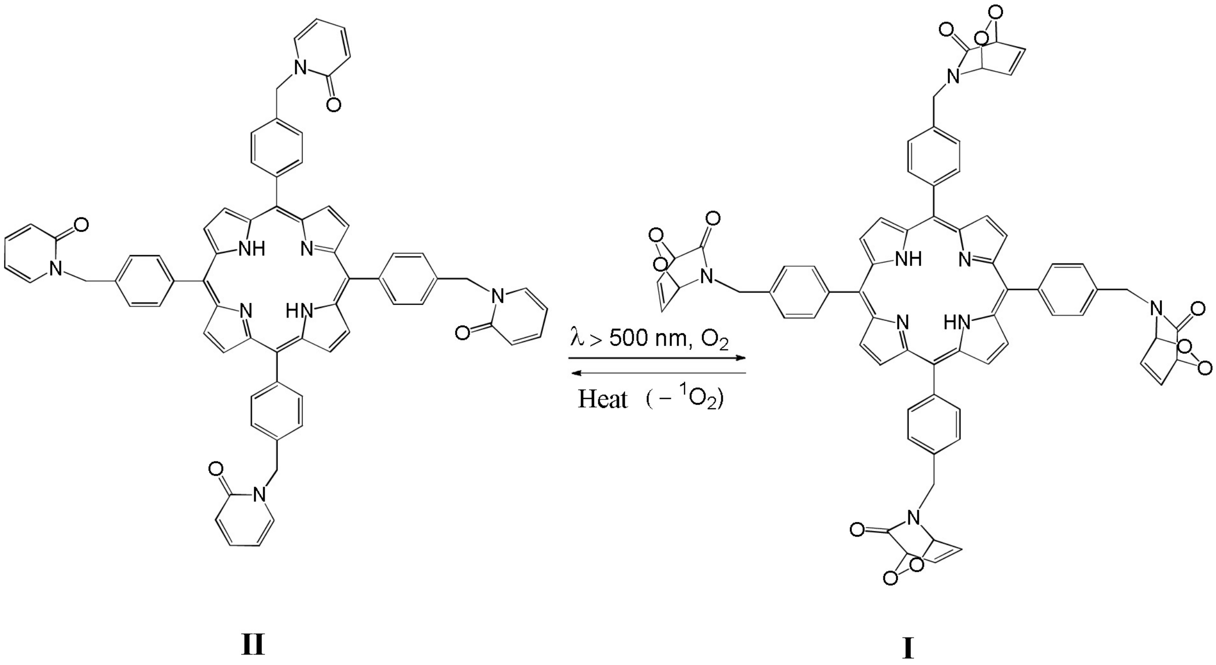

Fig. 1. Reversible generation, trap, and release of singlet oxygen by **II**.

simulant, 2-chloroethyl ethyl sulfide (CEES), by singlet oxygen released in the dark from the sensitizer-storage molecule is demonstrated.

2. Materials

As depicted in Fig. 2, the 2-pyridone linked porphyrin **II** was synthesized under anhydrous conditions by reacting 5,10,15,20-tetrakis(α-bromo-p-tolyl)porphyrin (**III**) for 4 h with 2-hydroxypyridine (2-pyridone tautomer) in the presence of NaH in refluxing THF. Solid remaining in the bottom of the reaction vessel was filtered and washed with dichloromethane. The filtrate was concentrated and a purple solid was recovered. The solid was analyzed by ^{1}H NMR in DMSO-d$_6$ and confirmed to be the pyridone linked tetraphenylporphyrin. The ^{1}H NMR spectrum of the purple solid shows a broad singlet (2H) upfield at δ −2.81 which is characteristic absorption by the porphyrin N—H. The most downfield singlet (8H) at δ 8.82 is assigned to the pyrrolic protons. Two doublets at δ 7.68 (8H, d; J = 7.58 Hz) and δ 8.19 (8H, d; J = 7.58 Hz) correspond to the ortho- and meta-phenyl ring protons of the porphyrin, respectively. Absorptions at δ 6.37 (t, 4 H; J = 6.82 Hz), 6.79 (d, 4 H; J = 9.09 Hz), 7.48 (t, 4 H; J = 9.09 Hz) and 7.63 (d, 4 H; J = 6.82 Hz) are due to the pyridone ring protons. The singlet at δ 5.54 (8H) which corresponds to the methylene protons on the link between the phenyl group and the pyridone nitrogen is key to establishing the final product. In porphyrin **III** the methylene protons appear as a singlet at 4.85 ppm [6]. The downfield shift to 5.54 ppm after coupling, with no residual signal at 4.85 ppm, indicates that coupling occurs at all four tolyl sites of the porphyrin [5].

Porphyrin **II** was synthesized by condensing α-bromo-p-tolualdehyde (**IV**) with pyrrole in the presence of amberlyst ion-exchange catalyst in dry chloroform according to the method of Lindsey et al. [7]. The aldehyde and pyrrole were allowed to react for 5 h at room temperature before the oxidant, 2,3-dichloro-5,6-dicyanobenzoquinone (DDQ), was added. After 40 min the reaction mixture was filtered through a short column of neutral alumina. The eluted solution was concentrated to yield a purple solid that was characterized by a single TLC spot. ^{1}H NMR signals agreed with the values reported by Fukushima et al. [6]. The aldehyde precursor **IV** was formed by reducing the nitrile group of α-bromo-p-tolunitrile (**V**) with diisobutylaluminum hydride (DIBAL-H) in dry toluene, followed by acid catalyzed hydrolysis [6].

3. Methods

UV–vis absorption spectra were obtained with a Shimadzu UV2100U spectrometer. Fluorescence spectra were measured with a Perkin-Elmer LS 50 B luminescence spectrometer outfitted with a R928 phototube. Fluorescence quantum yields were determined by the comparison method using the free base of 5,10,15,20-tetraphenylporphyrin (H_2TPP) as the standard [9]. Fluorescence lifetimes were measured with a Photon Technology International TM-3 time resolved spectrometer with dye laser excitation. Proton ^{1}H NMR spectra were recorded with a Bruker Avance 400 MHz instrument using chloroform-d solvent. Endoperoxide moieties in **I** were generated by irradiating chloroform-d solutions of **II** with the output of a 150 W xenon arc lamp passed through a yellow cutoff (500 nm) glass filter. Irradiations were performed with a fine stream of O_2 bubbling through the solutions. For the dark reaction of CEES with singlet oxygen generated from the thermal degradation of **I** to form **II**, 15.7 mg of **II** was dissolved in chloroform-d and irradiated in an NMR tube with bubbling oxygen until NMR spectra indicated complete conversion of **II** to **I**. To this solution, 1.8 μL of CEES was added under subdued room light. The solution was then wrapped in aluminum foil to keep it from exposure to light. The NMR spectrum was recorded immediately and it showed no indication that any reaction of CEES had taken place.

Theoretical calculations were carried out using the Gaussian 09 program [8]. Solvent effects were included using the Self-Consistent Reaction Field (SCRF) Polarizable Continuum Model (PCM) options within the program.

4. Results and discussion

4.1. Spectroscopic properties

The UV–vis absorption spectrum of **II** in chloroform has characteristic porphyrin Soret and Q-bands similar in position and relative

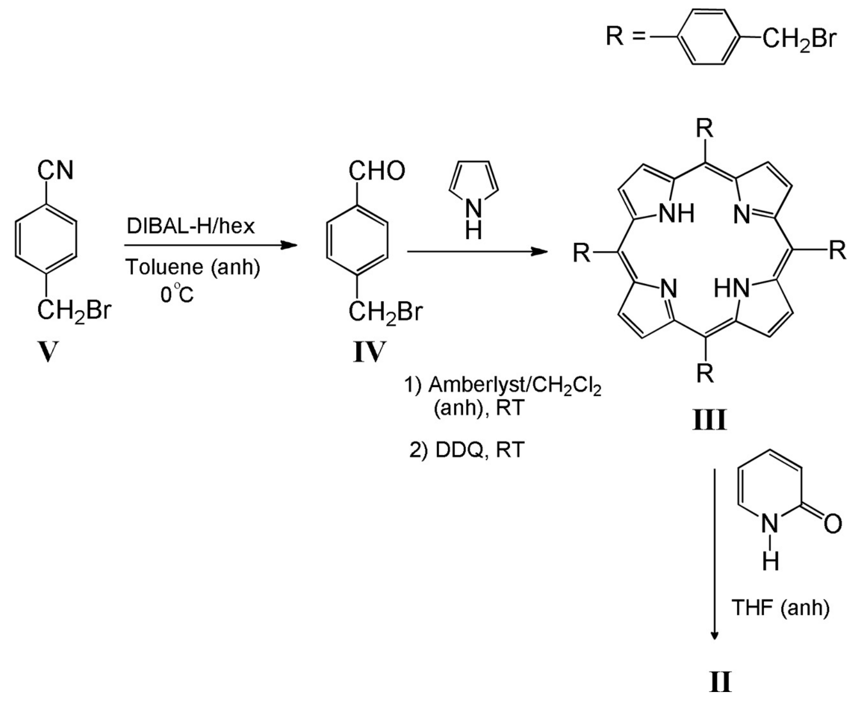

Fig. 2. Reaction scheme for the preparation of **II**.

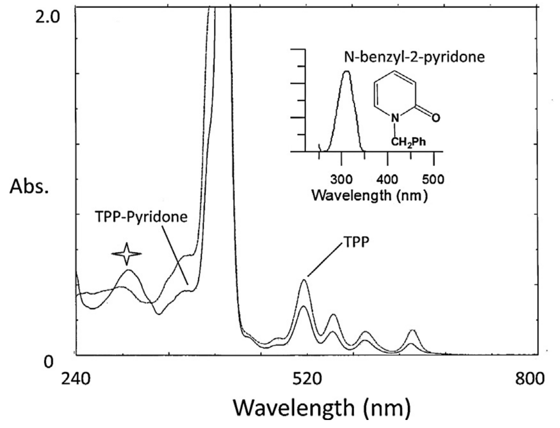

Fig. 3. UV–vis absorption spectra of **II** and of H_2TPP in chloroform. The star indicates the 296 nm band assigned to absorption by the 2-pyridone moieties in **II**. For comparison, the inset shows the absorption spectrum of N-benzyl-2-pyridone.

intensity to those of H_2TPP (Fig. 3). The absorption spectrum of **II** also exhibits an absorption band in the UV region with a maximum at 296 nm. Because of its similarity to the absorption spectrum of N-benzyl-2-pyridone in chloroform (see inset, Fig. 3), the 296 nm band is assigned to absorption by the 2-pyridone moieties in **II**. The fluorescence and excitation spectra of **II** in chloroform are also similar to those of H_2TPP. Photophysical properties of **II** were also measured. The fluorescence quantum yield of **II** in chloroform was determined to be 0.11, which is identical to the value that has been reported for H_2TPP [9]. Fluorescence lifetimes in degassed chloroform were measured in our laboratory to be 9.66 ± 0.13 ns for **II** and 9.93 ± 0.08 ns for H_2TPP. Thus, the electronic spectral and photophysical properties fail to reveal any significant π–π perturbation between the porphyrin and 2-pyridone ring systems. The methylene spacer appears to be effective in isolating the two units.

4.2. Cyclic irradiation of *I* in the presence of oxygen

A solution of **II** in chloroform was irradiated for 20 min in the presence of a fine stream of O_2 gas at ambient temperature. A comparison of ^{1}H NMR spectra before and after irradiation indicates approximately 90% consumption of the pyridone moieties accompanied by the formation of new proton signals. By comparison with the known ^{1}H NMR spectrum of the endoperoxide of N-benzyl-2-pyridone [5], the new signals that arise after irradiation are attributed to formation of the corresponding endoperoxides

Table 1
Experimental and computed activation parameters for the decomposition of endoperoxides **I** and N-benzyl-2-pyridone.

Reaction	Method	$\Delta H^{\ddagger}$(kcal/mol)	$\Delta G^{\ddagger}$(kcal/mol)
A.	NMR	26.7	24.0
B.	NMR	26.3	24.2
	DFT (B3LYP/6-311 + G*)	21.6	22.1
A.	**I** → **II** + $^1O_2$		
B.	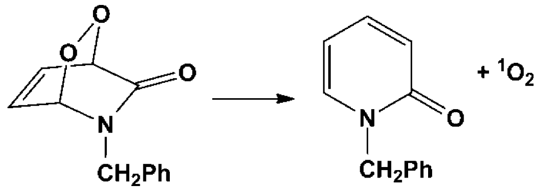		

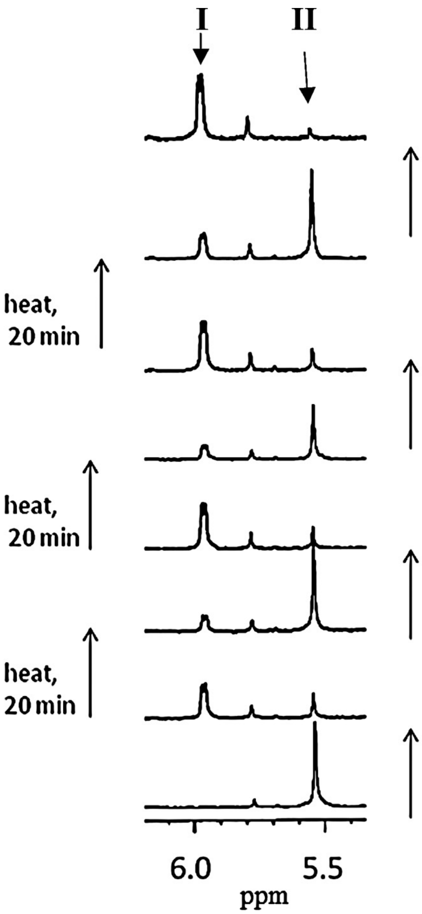

Fig. 4. ^{1}H NMR spectra showing the reversible cycling between **II** and **I**. The out-of-phase growth and reduction of NMR peaks assigned to compound **II** (5.54 ppm) and compound **I** (5.97 ppm) after cycles of irradiation and heating is clearly evident.

derived from oxidation of the pyridone moieties in **II** by singlet oxygen. Heating the solution to 40 °C after irradiating them and maintaining the temperature there for 20 min resulted in a reduction of the signals from the endoperoxide moieties and a recovery of signals from the pyridone moieties. The irradiation-heating experiment was repeated for three cycles. The NMR overlay spectra in Fig. 4 demonstrate reversible trapping and releasing of singlet oxygen throughout these cycles without detectable decomposition or side reactions.

Kinetics of endoperoxide decomposition were measured by monitoring the decay of the endoperoxide NMR signal as a function of time at several fixed temperatures between 25 and 50 °C. The decay data followed first-order kinetics throughout, as shown in Fig. 5. Thermodynamic activation parameters for the thermolysis reaction were determined from an Eyring plot (Fig. 6) of the kinetic data. It is seen from Table 1 that the values obtained are close to values we measured for the related model compound, N-benzyl-2-pyridone, under identical conditions. Just as the spectroscopic and photophysical properties associated with the porphyrin moiety are not perturbed by the presence of the pyridone ring, the kinetic properties of the endoperoxide decomposition are not significantly altered by the presence of the porphyrin ring.

*4.3. Dark reaction of CEES with singlet oxygen generated from thermal decomposition of **I***

A solution of CEES and **I** in chloroform-d prepared as described in the Methods section was allowed to sit in the dark for several

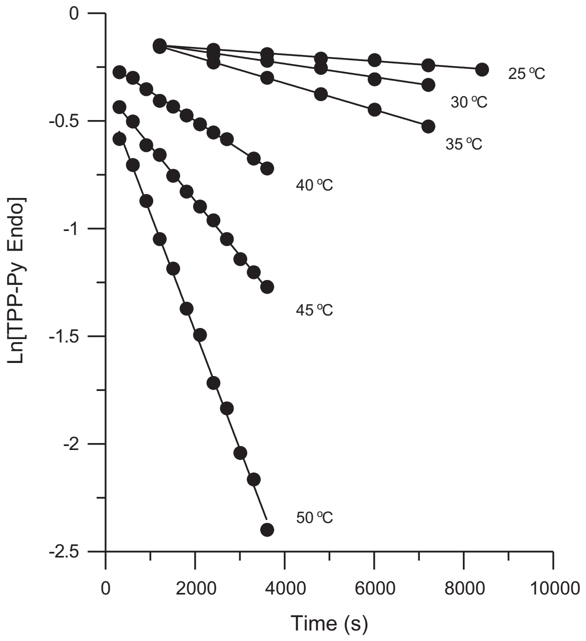

Fig. 5. Kinetics of endoperoxide decomposition were measured by monitoring the decay of the ^{1}H-NMR signal of **I** as a function of time at several fixed temperatures between 25 and 50 °C. The linearity of the first-order plots demonstrates that the decay data follow first-order kinetics throughout.

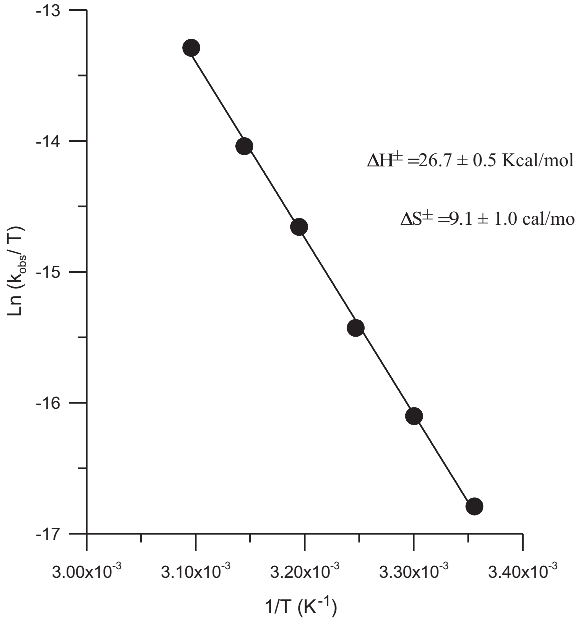

Fig. 6. Eyring plot of rate constants derived from the data presented in Fig. 5.

hours at room temperature. The NMR spectrum was rerecorded and no change was apparent. After heating the solution to 40 °C and holding at this temperature for 10 min, all done in the dark, clear evidence of the buildup of CEES degradation products [2] are seen in the ^{1}H NMR spectrum, shown (in part) Fig. 7. This preliminary study of a dark reaction of **I** will be followed up by more extensive studies in the future. However, it does demonstrate the potential for molecules that generate, trap, store, and release singlet oxygen to be used in various applications.

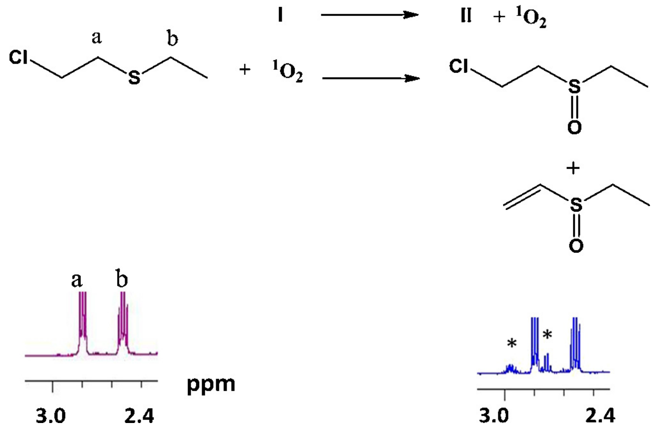

Fig. 7. NMR spectra of CEES and oxidized products formed by the reaction of CEES with singlet oxygen released by **I**.

4.4. Computations

Wasserman et al. [10] have demonstrated that calculations carried out at the B3LYP/6-311 + G* level of theory provides a reasonable approach for studying the energetics of the decomposition of endoperoxides of substituted naphthalenes to yield singlet oxygen and the parent naphthalene. Under the assumption that the H_2TPP moiety exerts a minor influence, the energetics of the thermolysis of **I** was approximated by a computational study of the simpler molecule N-benzyl-2-pyridone and its endoperoxide using the methods reported previously [10]. Geometry optimizations at the B3LYP/6-311 + G* level were performed for N-benzyl-2-pyridone and the endoperoxide adduct modeled in a chloroform environment using the Self-Consistent Reaction Field (SCRF) Polarizable Continuum Model (PCM) options. Minimum energy structures were confirmed by obtaining all positive frequencies for the calculated normal modes of vibration. Zero-point energy corrections were applied to the computed energies. The transition state structure associated with the decomposition of the endoperoxide to N-benzyl-2-pyridone and singlet oxygen was characterized by one negative vibration that corresponds to oscillation between the reactant and product side of the reaction coordinate. Following Wasserman et al. [10], the energy of singlet oxygen was estimated to be −150.32792 H. As shown in Table 1, the agreement between the experimental activation parameters and the DFT calculated values is reasonable and typical for this approach [10].

5. Conclusion

A new molecule, **II,** that has H_2TPP linked with four 2-pyridone moieties has been synthesized and shown to reversibly generate, trap, store, and release singlet oxygen. The use of this material as a source of singlet oxygen in the absence of light has been demonstrated by the dark oxidation of CEES. Kinetic data for the decay of the endoperoxide adduct, **I**, show first-order behavior between 25 °C and 50 °C. Further applications of this and related materials are in progress.

Acknowledgements

This work was supported by the U.S. Department of Defense under Army contracts W911NF-04-C-0081 and W911NF-07-D-0001 as well as by Air Force contracts W911QY-10C-0181 and W911QY-10-C-018. Dr. Joseph Wander from the Airbase Technologies Division (AFRL/RXQ) of the U.S. Air Force Research Laboratory is thanked for his technical insight provided during numerous discussions. In addition, we appreciate Dr. Heidi Schreuder-Gibson of the U.S. Army Natick Soldier RDE Center for her interest and stimulating conversations throughout this effort.

References

[1] M.C. DeRosa, R.J. Crutchley, Coordination Chemistry Reviews 233–234 (2002) 351.
[2] A. Toutchkine, E.L. Clennan, Tetrahedron Letters 40 (1999) 6519.
[3] K.I. Salokhiddinov, I.M. Byteva, G.P. Gurinovich, Journal of Applied Spectroscopy 34 (1981) 561.
[4] J.-M. Aubry, C. Pierlot, J. Rigaudy, R. Schmidt, Accounts of Chemical Research 36 (2003) 668.
[5] M. Matsumoto, M. Yamada, N. Watanabe, Chemical Communications (2005) 483.
[6] H. Fukushima, D.M. Taylor, H. Morgan, Langmuir 11 (1995) 3523.
[7] J.S. Lindsey, I.C. Schreiman, H.C. Hsu, P.C. Kearney, A.M. Marguerettaz, Journal of Organic Chemistry 52 (1987) 827.
[8] M.J. Frisch, G.W. Trucks, H.B. Schlegel, G.E. Scuseria, M.A. Robb, J.R. Cheeseman, G. Scalmani, V. Barone, B. Mennucci, G.A. Petersson, H. Nakatsuji, M. Caricato, X. Li, H.P. Hratchian, A.F. Izmaylov, J. Bloino, G. Zheng, J.L. Sonnenberg, M. Hada, M. Ehara, K. Toyota, R. Fukuda, J. Hasegawa, M. Ishida, T. Nakajima, Y. Honda, O. Kitao, H. Nakai, T. Vreven, J.A. Montgomery Jr., J.E. Peralta, F. Ogliaro, M. Bearpark, J.J. Heyd, E. Brothers, K.N. Kudin, V.N. Staroverov, R. Kobayashi, J. Normand, K. Raghavachari, A. Rendell, J.C. Burant, S.S. Iyengar, J. Tomasi, M. Cossi, N. Rega, J.M. Millam, M. Klene, J.E. Knox, J.B. Cross, V. Bakken, C. Adamo, J. Jaramillo, R. Gomperts, R.E. Stratmann, O. Yazyev, A.J. Austin, R. Cammi, C. Pomelli, J.W. Ochterski, R.L. Martin, K. Morokuma, V.G. Zakrzewski, G.A. Voth, P. Salvador, J.J. Dannenberg, S. Dapprich, A.D. Daniels, O. Farkas, J.B. Foresman, J.V. Ortiz, J. Cioslowski, D.J. Fox, Gaussian 09. Revision A. 02, Gaussian, Inc., Wallingford, CT, 2009.
[9] M. Gouterman, G.E. Khalil, Journal of Molecular Spectroscopy 53 (1974) 88.
[10] H.H. Wasserman, K.B. Wiberg, D.L. Larsen, J. Parr, Journal of Organic Chemistry 70 (2005) 105.